Communication

High–Efficiency, Widely Tunable MgO: PPLN Optical Parametric Oscillator

Yueyue Lian [1], Wenlong Tian [1,*], Hao Sun [1], Yang Yu [2], Yulong Su [1], Hui Tong [1], Jiangfeng Zhu [1] and Zhiyi Wei [3]

[1] School of Optoelectronic Engineering, Xidian University, Xi'an 710071, China; lillian-yue@stu.xidian.edu.cn (Y.L.); sunhao6@stu.xidian.edu.cn (H.S.); ylsu@xidian.edu.cn (Y.S.); tonghui@xidian.edu.cn (H.T.); jfzhu@xidian.edu.cn (J.Z.)

[2] Academy of Advanced Interdisciplinary Research, Xidian University, Xi'an 710071, China; yangyu@xidian.edu.cn

[3] Beijing National Laboratory for Condensed Matter Physics, Institute of Physics, Chinese Academy of Sciences, Beijing 100190, China; zywei@iphy.ac.cn

* Correspondence: wltian@xidian.edu.cn

Abstract: We report on the investigation of a high–efficiency, widely tunable femtosecond optical parametric oscillator (OPO) based on a multi–period MgO–doped periodically poled lithium niobite (MgO: PPLN) crystal, pumped by an all–solid–state femtosecond mode–locked Yb: KGW laser at 1030 nm providing 100 fs pulses. With 6 W pump power, the OPO generates 2.68 W of signal power at 1540 nm and 1.2 W of idler power at 3110 nm, which corresponds to the total conversion efficiency adding up to 67.4%. To the best of our knowledge, this is the highest conversion efficiency of a femtosecond OPO. Meanwhile, in order to obtain a broad optical spectrum range, both the grating period and working temperature are tuned, resulting in tunable signals of 1.43–1.78 μm and idlers of 2.44–3.68 μm. This source will be used to generate a femtosecond mid–infrared laser of wavelength range 3.7–6.5 μm and tens milliwatts average power through difference frequency generation (DFG).

Keywords: nonlinear frequency conversion; femtosecond optical parametric oscillator; difference frequency generation; MgO–doped periodically poled lithium niobite

1. Introduction

Broadband femtosecond mid–infrared (mid–IR) sources play an important role in various applications, such as environmental monitoring, medical diagnosis, spectral analysis, trace gas detections, etc. [1,2]. Commonly available mid–IR laser sources can be divided into four main categories: gas lasers, semiconductor lasers, solid–state lasers and frequency conversion–based laser sources [3]. Due to the lack of mature laser gain media with emission in the mid–IR, parametric down–conversion of near–infrared (near–IR) sources through optical parametric oscillators (OPO), optical parametric amplifiers (OPA) or difference–frequency generation (DFG) remain the most efficient approaches to obtain high–power and widely tunable femtosecond mid–IR lasers [4–7]. Nowadays, there is a vast variety of research works on the generation of mid–IR lasers by parametric conversion, including intra–pulse difference frequency generation (IPDFG) [8], DFG using a dual–signal–wavelength OPO [9], and DFG between the signal and idler wavelengths of an OPA or OPO [10,11], as well as supercontinuum–seeded DFGs [12,13].

In 2020, Florian Mörz et al. presented a dual OPO/OPA DFG method based on two independently tunable input lasers, provided by two synchronously pumped parametric seeding units. They compared this method to the traditional DFG approach of mixing the signal and idler beams from a single OPA or OPO (signal–idler DFG). In this work, they demonstrated that the output power and photon efficiency of the DFG wavelength under 10 μm generated by the signal–idler DFG are higher than that of dual OPO/OPA DFG [10]. Taking the much simpler configuration of the signal–idler DFG method into consideration,

this approach is a very suitable option for generating tunable 4–7 μm femtosecond lasers with tens of milliwatts average power [11].

At present, several groups have shown research results of femtosecond OPOs that output both signals and idlers simultaneously [14–18]. In 2018, Xianghao Meng et al. presented KTA–OPO pumped by a Yb femtosecond laser. At the pump power of 7 W, the OPO generates 2.32 W of signal power at 1.55 μm, corresponding to 1.31 W of idler power at 3.05 μm [17]. Although it has a high output power, the pump threshold of the KTA–OPO is as high as 3.11 W. Due to the substantially larger effective nonlinear coefficient of MgO: PPLN, it is easier to achieve a higher conversion efficiency as well as lower threshold compared to a KTA crystal [19,20]. As a result, we choose the OPO system based on a MgO: PPLN crystal to generate signals and idlers of high average power at the same time. The proposal is depicted in Figure 1. Pumped by a commercial high–power femtosecond Yb laser, the MgO: PPLN OPO system is able to generate a tunable signal wavelength range cover of 1.4–1.8 μm and a tunable idler range of 2.4–3.9 μm with Watt–level average output power based on our design. Then, using a time–delay device and a beam combination mirror, the signal and idler are poured into the DFG stage together. The signal and idler beam from OPO can serve as the pump and signal laser of the DFG, respectively, so a mid–IR wavelength range of 4–7 μm can be obtained. Wavelength tuning is achieved by using the tunable signals and idlers and rotating the crystal angle accordingly for satisfying the phase matching condition of the DFG process.
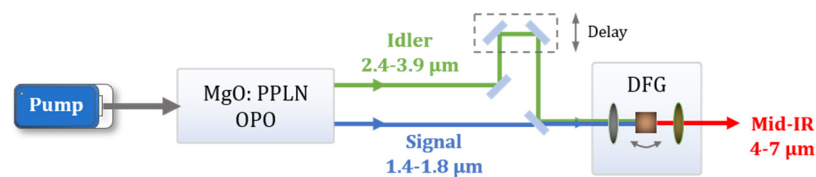

Figure 1. Proposal for different frequency generation into the mid–IR spectral region.

In this work, we focus on the investigation of the high–conversion efficiency broadband tunable femtosecond MgO: PPLN OPO. By varying the grating period and working temperature of the crystal while optimizing the cavity length, a tunable signal wavelength range of 1.43–1.78 μm is produced, which corresponds to a tunable idler range of 2.44–3.68 μm. Furthermore, using a 15% output coupler, a maximum output power of 2.68 W is obtained at 1540 nm and 1.2 W of idler power at 3110 nm, where the total conversion efficiency adds up to 67.4%.

2. Experimental Setup

The experimental setup of the femtosecond MgO: PPLN OPO is sketched in Figure 2. The pump source is a commercial femtosecond mode–locked Yb: KGW laser delivering 100 fs pulses at a 75.5 MHz repetition rate with 6 W average power. The pump beam passes a half–wave plate (HWP1) and a polarizing beam splitter (PBS), which allow the pump power to be controlled for the OPO stage. The second half–wave plate (HWP2) is used to adjust the polarization of the pump for satisfying the phase matching condition. A lens (L1) with a focal length of 75 mm is chosen so that the beam waist diameter at the focusing point in the MgO: PPLN crystal is about 72 μm. The corresponding maximum peak intensity is about 19.5 GW/cm^2. In addition, the transverse mode size of the OPO resonant cavity is 80 μm, which is beneficial in terms of achieving better mode matching.
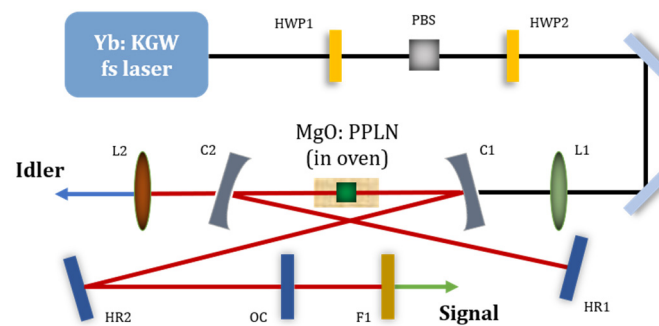
Figure 2. Schematic of the experimental setup for widely tunable MgO: PPLN femtosecond OPO. HWP1, HWP2: half–wave plates; PBS: polarizing beam splitter; L1, L2: lenses; C1, C2: concave spherical mirrors; HR1, HR2: plane high–reflection mirrors; OC: plane output coupler; F1: long–wave filter.

The signal single–resonant OPO consists of two concave mirrors (C1, C2), two high–reflection mirrors (HR1, HR2) and a plane output coupler (OC). The C1 and C2 are coated to support high transmission of the pump at 1030 nm and high reflection for the signal at 1.4–1.7 μm, and their radii of curvature are both 100 mm. In addition, C2 provides high transmission (T > 95%) for the idler in the range of 2.5–4.5 μm. The two high–reflection mirrors also provide high reflection for the signal at 1.23–1.73 μm and 1.41–1.83 μm, respectively. Two output coupler mirrors are used, one of which has a transmittance of 1.5% in the 1.22–1.74 μm range and the other has a transmittance of 15% at 1.4–1.8 μm.

The crystal is a 1 mm long MgO: PPLN crystal of 1×6 mm^2 cross section containing 5 different grating periods of 29, 29.5, 30, 30.5 and 31 μm. The input and output facets of the crystal are coated with antireflection coatings at 1000–1100 nm (R < 1%), 1400–1900 nm (R < 1%) and 2300–4000 nm (R < 10%). The multi–period MgO: PPLN crystal is placed in a heating oven to conduct temperature tuning precisely from 25 °C to 250 °C with an accuracy of ±0.1 °C, which can also increase the damage threshold of PPLN with heating. A silicon filter lens (L2, f = 100 mm) that has a high transmission coating (T > 95%) at 2–5 μm is used to separate and collimate the generated idler from the residual pump. A long–wave filter (F1) is used to block unwanted parasitical SHG and SFG and penetrate signal wavelength only over 1366–2150 nm (T > 99%). The total cavity length of the OPO is set to 993 mm, corresponding to a repetition rate of 151 MHz, which is twice that of the Yb: KGW oscillator.

3. Experimental Results

When the cavity length of the MgO: PPLN OPO is accurately matched to half of the cavity length of the Yb: KGW laser, the stable output of the signal wave is achieved. Firstly, using a 1.5% output coupler, with the crystal with a poled period of 30.5 μm and crystal temperature of 25 °C, a signal of central wavelength at 1573.5 nm with the highest power of 1 W is generated. Correspondingly, the idler is centered at 2982 nm with 521 mW. Then, using a 15% output coupler, with the crystal with a poled period of 30 μm and crystal temperature at 75 °C, a signal of central wavelength at 1540 nm with the highest power of 2.68 W is generated. Correspondingly, the idler is centered at 3110 nm with 1.2 W. Figure 3a shows the variation in signal and idler output power versus the pump power. The pump threshold of the MgO: PPLN OPO is about 1.7 W. Considering that the silicon filter lens has only 95% transmittance in the idler tuning range and the actual effective pump laser power on MgO: PPLN crystal is only 5.85 W, the pump–to–signal power conversion is 45.8% and pump–to–idler power conversion is 21.6%, corresponding to a total conversion efficiency of 67.4%. We recorded the power stability of the signal radiation centered at 1540 nm for half an hour. The result is shown in Figure 3b, and the root mean square (RMS) power fluctuation is 0.6%. The power fluctuation can mainly be attributed to the change in laboratory environment and mechanical component.
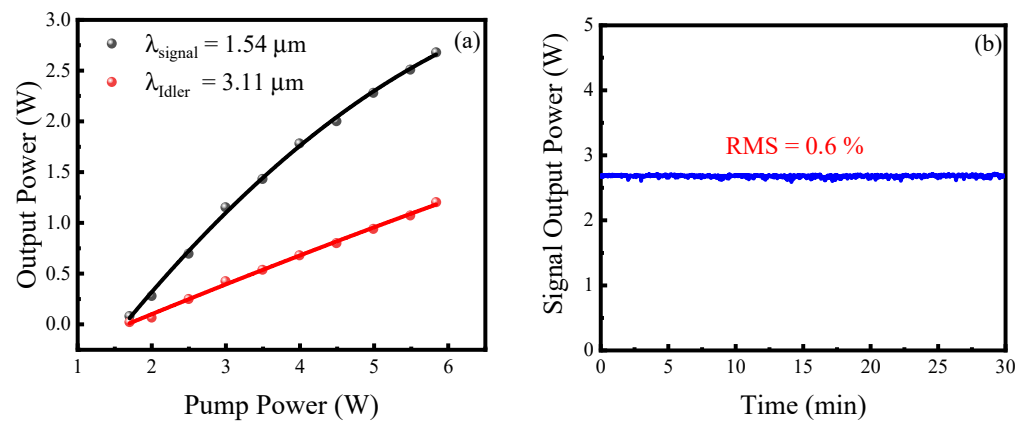
Figure 3. (**a**) Variation in the signal output power and idler output power as a function of the pump power. (**b**) The output power stability of signal radiation.

By varying the grating period and working temperature of the crystal while optimizing the cavity length, the signal wavelength can be tuned from 1.43 to 1.78 µm and the idler from 2.44 to 3.68 µm. Figure 4 illustrates the variation in the signal power and the idler power with wavelength when the pump is fixed at 6 W. The average power of the signal pulse in the tuning range of 1.43–1.70 µm exceeds 1.5 W, while the idler power exceeds 500 mW for the entire tuning range of 2.44–3.68 µm.
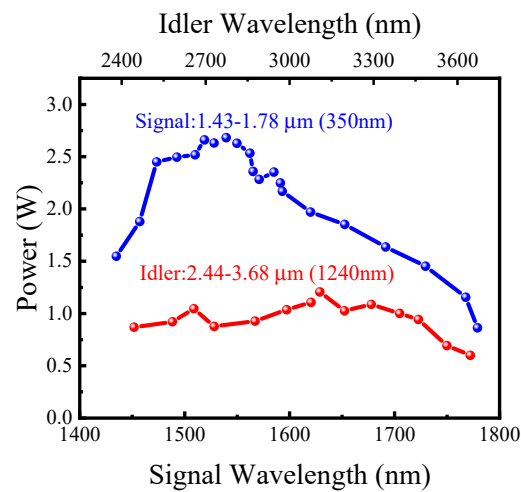

Figure 4. Signal and idler output powers of the entire tuning range at a fixed pump power.

We also measured the signal pulse width using a frequency–resolved optical gating (FROG) measurement device, with the results shown in Figure 5. Figure 5a,b is the original recorded and retrieved traces, respectively. Using an inverse algorithm, we obtained the spectrum and temporal pulse as shown in Figure 5c,d. As evident from Figure 5, the pulse duration of 214 fs is obtained at a signal of 1573.5 nm. The output signal temporal pulse sequence from OPO is given in Figure 6. As shown in the figure, although there is a difference in intensity between the two adjacent pulses, the difference is not significant.
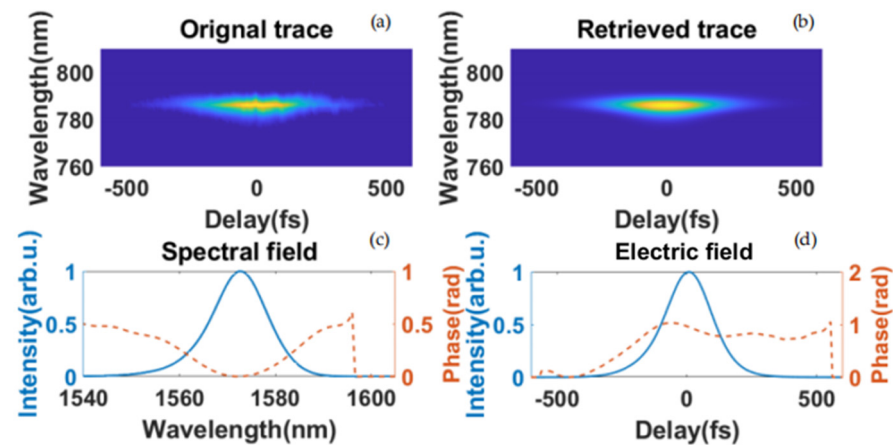
Figure 5. Measured and reconstructed traces and spectra from the FROG measurement. (**a**) is the FROG trace measured; (**b**) is the reconstructed trace; (**c**) is the reconstructed spectrum; (**d**) is the reconstructed time domain pulse; and the dashed lines in (**c**,**d**) are phase distributions.
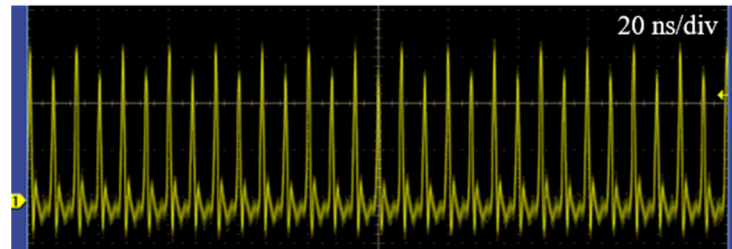

Figure 6. The output signal temporal pulse sequence of OPO.

When the grating period was 30.5 μm, 30.0 μm and 29.5 μm, respectively, by varying the crystal temperature from 25 to 200 °C and adjusting the cavity length to have the maximum signal output power, we recorded the wavelength tuning curves of signal and idler. As shown in Figure 7, the signal has a red shift with the increase in temperature, and the whole wavelength range is 1.48–1.73 μm. Correspondingly, the idler tunable range is 2.54–3.38 μm.
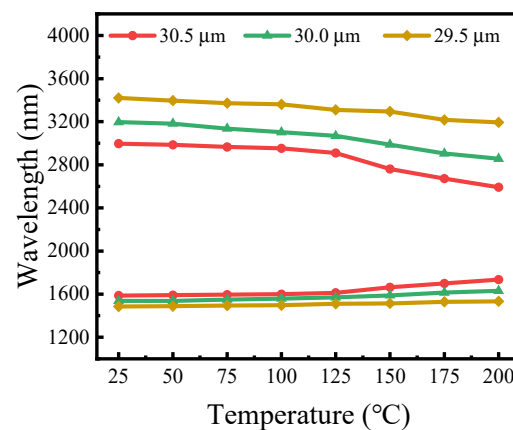

Figure 7. Wavelength tuning curves of signal and idler with different temperatures when grating period was 30.5 μm, 30.0 μm and 29.5 μm, respectively.

In addition, by varying the grating period and working temperature of the crystal while optimizing the cavity length, the signal radiation can be tuned continuously over 350 nm across 1.43–1.78 μm. The normalized output signal spectra in the tuning range are given in Figure 8a. It is noticeable that the range of the signal wavelength is limited

by the coating on the concave and plane mirrors. Figure 8b shows the typical normalized spectra of the idler, and the corresponding idler radiation is tunable over 1240 nm across 2.44–3.68 μm.
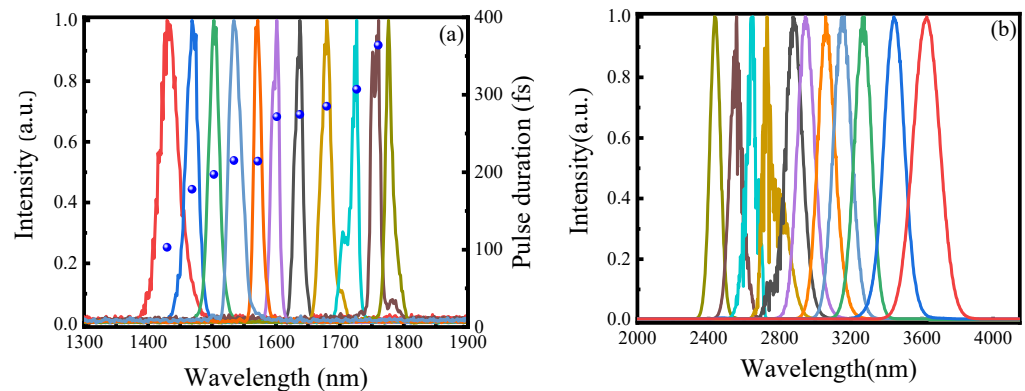

Figure 8. (**a**) The normalized output signal spectra in the tuning range of 1.43–1.78 μm and corresponding pulse duration of each spectrum (blue data spots). (**b**) The normalized output idler spectra in the tuning range of 2.44–3.68 μm.

We also studied the temporal characteristics of the OPO by measuring the pulse width of the signal radiation across the tuning range. As shown in Figure 8a, the measured pulse durations are in the range of 102–364 fs over the entire wavelength tuning ranges from 1430 nm to 1760 nm. It is found that the longer the signal wavelength is, the longer the pulse duration is. The increase in signal pulse width can be attributed to the increase in group velocity mismatch (GVM) among the interacting waves.

4. Conclusions and Discussion

In this paper, we report on a high–efficiency, widely tunable MgO: PPLN OPO pumped by a femtosecond mode–locked Yb: KGW laser at 75.5 MHz of 1030 nm central wavelength for widely tunable mid–IR DFG. The signal wavelength tunable from 1.43 to 1.78 μm together with the idler tunable from 2.44 to 3.68 μm at 151 MHz are obtained by varying the grating period and working temperature of the crystal while optimizing the cavity length. Using a 15% output coupler, a signal average output power of 2.68 W is obtained at 1540 nm and 1.2 W of idler power at 3110 nm. With 6 W pump power, the total conversion efficiency adds up to 67.4%. Such a high conversion efficiency is achieved firstly because the maximum peak intensity of the pump is 19.5 GW/cm^2 in this work, which can greatly promote the improvement of the conversion efficiency. In addition, for the experimental setup of the OPO, C2 provides high transmission (T > 95%) for the idler and the OC has a transmittance of 15% for signal, which results in more output power being extracted.

In addition, we investigated the conversion efficiency of femtosecond OPOs that can be used for signal idler DFG, and a summary of the research results is shown in Table 1. Among them, Jintao Fan et al. demonstrated a dielectric mirror–less OPO based on MgO: PPLN with a conversion efficiency of 40.2% in 2018. Although different wavelength components can be separated for the angular dispersion of the prism, the cavity losses are higher than that of the conventional dielectric mirror–based system, so the conversion efficiency is limited. In the same year, Xianghao Meng et al. presented a KTA–OPO with a conversion efficiency of 51.8%, which is due to the fact that the maximum peak intensity of the pump is 15.2 GW/cm^2 and a concave mirror with high transmission for the idler is adopted. However, the performance of the KTA crystal cannot support higher conversion efficiency. By comparison, in this work, we obtained the highest conversion efficiency of 67.4% in a similar OPO wavelength range, which benefits from high pump peak intensity and extractable power, as well as the larger effective nonlinear coefficient of MgO: PPLN. Then, we planned to use the signal and idler wavelengths of the synchronously pumped wide–tuning OPO for DFG. By calculating and simulating this, tens of milliwatts of average

power in the tunable spectral range of 3.7–6.5 μm will be achieved [21–25]. Such a high–efficiency broadband tunable near–mid–infrared femtosecond source is of importance for ultrafast spectroscopy and frequency comb generation.

Table 1. A summary of femtosecond OPO research results.

Year of Publication	Pump Source	OPO Crystal	Signal Power	Idler Power	Conversion Efficiency	Reference
2004	1030 nm 68 W	PPSLT	19 W @1.45 μm	7.8 W @3.57 μm	46.2%	[14]
2015	1035 nm 2 W	MgO: PPLN	355 mW @1628 nm	203 mW @2841.5 nm	31%	[15]
2018	1040 nm 4 W	MgO: PPLN	1.2 W @1482 nm	411 mW @3487 nm	40.2%	[16]
2018	1030 nm 7 W	KTA	2.32 W @1.55 μm	1.31 W @3.05 μm	51.8%	[17]
2021	1030 nm 7 W	KTP	2.05 W @1.53 μm	1.03 W @3.17 μm	44%	[18]
2022	1030 nm 6 W	MgO: PPLN	2.68 W @1540 nm	1.2 W @3110 nm	67.4%	This work

References

1. Tittel, F.K.; Richter, D.; Fried, A. Mid–Infrared Laser Applications in Spectroscopy. In *Solid–State Mid–Infrared Laser Sources*; Springer: Berlin/Heidelberg, Germany; Houston, TX, USA, 2003; Volume 89, pp. 458–529.
2. Ebrahim–Zadeh, M.; Sorokina, I.T. Mid–infrared coherent sources and applications. In *NATO Science for Peace and Security Series B: Physics and Biophysics*; Springer Science & Business Media: Berlin, Germany, 2008; p. XVIII 626.
3. Krzempek, K.; Sobon, G.; Abramski, K.M. DFG–based mid–IR generation using a compact dual–wavelength all–fiber amplifier for laser spectroscopy applications. *Opt. Express* **2013**, *21*, 20023–20031. [CrossRef] [PubMed]
4. Peng, Y.; Wei, X.; Wang, W.; Li, D. High–power 3.8 μm tunable optical parametric oscillator based on PPMgO: CLN. *Opt. Commun.* **2010**, *283*, 4032–4035. [CrossRef]
5. Sánchez, D.; Hemmer, M.; Baudisch, M.; Zawilski, K.; Schunemann, P.; Hoogland, H.; Holzwarth, R.; Biegert, J. Broadband mid–IR frequency comb with $CdSiP_2$ and $AgGaS_2$ from an Er, Tm: Ho fiber laser. *Opt. Lett.* **2014**, *39*, 6883–6886. [CrossRef] [PubMed]
6. Peng, Y.; Wei, X.; Luo, X.; Nie, Z.; Peng, J.; Wang, Y.; Shen, D. High–power and widely tunable mid–infrared optical parametric amplification based on PPMgLN. *Opt. Lett.* **2016**, *41*, 49–51. [CrossRef]
7. Erny, C.; Moutzouris, K.; Biegert, J.; Kühlke, D.; Adler, F.; Leitenstorfer, A.; Keller, U. Mid–infrared difference–frequency generation of ultrashort pulses tunable between 3.2 and 4.8 μm from a compact fiber source. *Opt. Lett.* **2007**, *32*, 1138–1140. [CrossRef]
8. Gaida, C.; Gebhardt, M.; Heuermann, T.; Stutzki, F.; Jauregui, C.; Antonio–Lopez, J.; Schülzgen, A.; Amezcua–Correa, R.; Tünnermann, A.; Pupeza, I.; et al. Watt–scale super–octave mid–infrared intrapulse difference frequency generation. *Light Sci. Appl.* **2018**, *7*, 94. [CrossRef]
9. Hegenbarth, R.; Steinmann, A.; Sarkisov, S.; Giessen, H. Milliwatt–level mid–infrared (10.5–16.5 μm) difference frequency generation with a femtosecond dual–signal–wavelength optical parametric oscillator. *Opt. Lett.* **2012**, *37*, 3513–3515. [CrossRef]
10. Mörz, F.; Steinle, T.; Linnenbank, H.; Steinmann, A.; Giessen, H. Alignment–free difference frequency light source tunable from 5 to 20 μm by mixing two independently tunable OPOs. *Opt. Express* **2020**, *28*, 11883–11891. [CrossRef]
11. Steinle, T.; Mörz, F.; Steinmann, A.; Giessen, H. Ultra–stable high average power femtosecond laser system tunable from 1.33 to 20 μm. *Opt. Lett.* **2016**, *41*, 4863–4866. [CrossRef]

12. Keilmann, F.; Amarie, S. Mid–infrared frequency comb spanning an octave based on an Er fiber laser and difference–frequency generation. *J. Infrared Millim. Terahertz Waves* **2012**, *33*, 479–484. [CrossRef]
13. Hegenbarth, R.; Steinmann, A.; Tóth, G.; Hebling, J.; Giessen, H. Two–color femtosecond optical parametric oscillator with 1.7 W output pumped by a 7.4 W Yb: KGW laser. *J. Opt. Soc. Am. B* **2011**, *28*, 1344–1352. [CrossRef]
14. Südmeyer, T.; Innerhofer, E.; Brunner, F.; Paschotta, R.; Usami, T.; Ito, H.; Kurimura, S.; Kitamura, K.; Hanna, D.C.; Keller, U. High–power femtosecond fiber–feedback optical parametric oscillator based on periodically poled stoichiometric $LiTaO_3$. *Opt. Lett.* **2004**, *29*, 1111–1113. [CrossRef] [PubMed]
15. Tian, W.L.; Wang, Z.H.; Zhu, J.F.; Wei, Z.Y. Tunable femtosecond near–infrared source based on a Yb: LYSO–laser–pumped optical parametric oscillator. *Chin. Phys. B* **2015**, *25*, 014207. [CrossRef]
16. Fan, J.; Gu, C.; Zhao, J.; Liao, R.; Chu, Y.; Chai, L.; Wang, C.; Hu, M. Dielectric–mirror–less femtosecond optical parametric oscillator with ultrabroad–band tunability. *Opt. Lett.* **2018**, *43*, 2316–2319. [CrossRef] [PubMed]
17. Meng, X.; Wang, Z.; Tian, W.; He, H.; Fang, S.; Wei, Z. Watt–level widely tunable femtosecond mid–infrared $KTiOAsO_4$ optical parametric oscillator pumped by a 1.03 μm Yb: KGW laser. *Opt. Lett.* **2018**, *43*, 943–946. [CrossRef] [PubMed]
18. Meng, X.; Wang, Z.; Tian, W.; Song, J.; Wang, X.; Zhu, J.; Wei, Z. High average power 200 fs mid–infrared KTP optical parametric oscillator tunable from 2.61 to 3.84 μm. *Appl. Phys. B* **2021**, *127*, 129. [CrossRef]
19. Baudisch, M.; Hemmer, M.; Pires, H.; Biegert, J. Performance of MgO: PPLN, KTA, and $KNbO_3$ for mid–wave infrared broadband parametric amplification at high average power. *Opt. Lett.* **2014**, *39*, 5802–5805. [CrossRef]
20. Aadhi, A.; Samanta, G.K. High power, high repetition rate, tunable broadband mid–IR source based on single–pass optical parametric generation of a femtosecond laser. *Opt. Lett.* **2017**, *42*, 2886–2889. [CrossRef]
21. Chang, J.H.; Mao, Q.H.; Feng, S.J.; Jiang, J.; Li, X.L.; Tian, Y.Y.; Xu, C.Q.; Liu, W.Q. Theoretical and experimental investigations of the Mid–IR DFG tuning property based on fiber laser fundamental lights. *Appl. Phys. B* **2011**, *104*, 851–859. [CrossRef]
22. Yanagawa, T.; Kanbara, H.; Tadanaga, O.; Asobe, M.; Suzuki, H.; Yumoto, J. Broadband difference frequency generation around phase–match singularity. *Appl. Phys. Lett.* **2005**, *86*, 161106. [CrossRef]
23. Cao, Q.; Kärtner, F.X.; Chang, G. Towards high power longwave mid–IR frequency combs: Power scalability of high repetition–rate difference–frequency generation. *Opt. Express* **2020**, *28*, 1369–1384. [CrossRef] [PubMed]
24. Burgess, I.B.; Rodriguez, A.W.; McCutcheon, M.W.; Bravo–Abad, J.; Zhang, Y.; Johnson, S.G. Difference–frequency generation with quantum–limited efficiency in triply–resonant nonlinear cavities. *Opt. Express* **2009**, *17*, 9241–9251. [CrossRef] [PubMed]
25. Suh, W.; Wang, Z.; Fan, S. Temporal coupled–mode theory and the presence of non–orthogonal modes in lossless multimode cavities. *IEEE J. Quantum Electron.* **2004**, *40*, 1511–1518.